

Ursa Major III/UNIONS 1: the darkest galaxy ever discovered?

Raphaël Errani,^{1,2} Julio F. Navarro,³ Simon E. T. Smith,³ and Alan W. McConnachie^{4,3}

¹McWilliams Center for Cosmology, Department of Physics, Carnegie Mellon University, Pittsburgh, PA 15213, USA

²Université de Strasbourg, CNRS, Observatoire Astronomique de Strasbourg, UMR 7550, F-67000 Strasbourg, France

³Department of Physics and Astronomy, University of Victoria, Victoria, BC V8P 5C2, Canada

⁴NRC Herzberg Astronomy and Astrophysics, 5071 West Saanich Road, Victoria, BC, V9E 2E7, Canada

Abstract

The recently-discovered stellar system Ursa Major III/UNIONS 1 (UMa3/U1) is the faintest known Milky Way satellite to date. With a stellar mass of $16_{-5}^{+6} M_{\odot}$ and a half-light radius of 3 ± 1 pc, it is either the darkest galaxy ever discovered or the faintest self-gravitating star cluster known to orbit the Galaxy. Its line-of-sight velocity dispersion suggests the presence of dark matter, although current measurements are inconclusive because of the unknown contribution to the dispersion of potential binary stars. We use N-body simulations to show that, if self-gravitating, the system could not survive in the Milky Way tidal field for more than a single orbit (roughly 0.4 Gyr), which strongly suggests that the system is stabilized by the presence of large amounts of dark matter. If UMa3/U1 formed at the centre of a $\sim 10^9 M_{\odot}$ cuspy LCDM halo, its velocity dispersion would be predicted to be of order $\sim 1 \text{ km s}^{-1}$. This is roughly consistent with the current estimate, which, neglecting binaries, places σ_{los} in the range 1 to 4 km s^{-1} . Because of its dense cusp, such a halo should be able to survive the Milky Way tidal field, keeping UMa3/U1 relatively unscathed until the present time. This implies that UMa3/U1 is in all likelihood the faintest and densest dwarf galaxy satellite of the Milky Way, with important implications for alternative dark matter models, and for the minimum halo mass threshold for luminous galaxy formation in the LCDM cosmology.

Keywords: Cold dark matter(265); Dwarf spheroidal galaxies(420); Low surface brightness galaxies(940); Milky Way Galaxy(1054); N-body simulations(1083); Star clusters(1567); Tidal disruption(1696)

1. Introduction

Ultra-faint dwarf galaxies (UFDs) are stellar systems with $M_{\star} < 10^5 M_{\odot}$, fainter than many globular clusters but gravitationally bound by the presence of large amounts of dark matter. They constitute direct probes not only of the formation mechanisms that govern the extreme faint-end of the galaxy luminosity function, but also of the structure of low-mass dark matter halos and, indirectly, of the nature of dark matter (see; e.g., Bullock & Boylan-Kolchin 2017; Simon 2019; Sales et al. 2022, for recent reviews).

The overall abundance of UFDs reflects the number of low-mass dark matter halos able to harbour luminous galaxies, placing important constraints on models where the physical nature of dark matter leads to the suppression of low-mass halos, such as in “warm dark matter” (WDM) (Bode et al. 2001; Lovell et al. 2014) or “fuzzy dark matter” (FDM) (Hu et al. 2000) models. For cold dark matter (CDM) models, where the number of low-mass halos is expected to be overwhelmingly larger than the number of UFDs, the abundance of faint systems probes the mass threshold between halos that remain “dark” (starless) and those massive enough for luminous galaxy

formation to proceed (Simon & Geha 2007; Ferrero et al. 2012; Peñarrubia et al. 2012; Fattahi et al. 2018).

This threshold is still being actively discussed, with some studies suggesting a relatively high virial¹ halo mass threshold ($\sim 10^9 M_{\odot}$) (Benitez-Llambay & Frenk 2020; Pereira-Wilson et al. 2023), determined primarily by the ability of hydrogen to cool in halos photo-heated by the ambient UV background (Efstathiou 1992; Quinn et al. 1996; Gnedin 2000), and other studies arguing for a much lower mass threshold, in order to accommodate the sheer number of observed UFDs plus those still likely missing from our currently incomplete inventory of Milky Way satellites (e.g., Nadler et al. 2021, and references therein).

In addition, because UFDs are physically small and heavily dark matter dominated, they probe the innermost regions of their dark matter halos, where competing dark matter models make differing predictions. Cold dark matter models predict “cuspy” density profiles (Navarro et al. 1996, 1997), which imply high average dark matter densities for UFDs. Cuspy

¹ Virial quantities are identified by a “200” subscript and defined at or within the virial radius, r_{200} , which encloses a mass a mean average density equal to 200× the critical density for closure. At $z = 0$, $\rho_{\text{crit}} = 3H_0^2 / (8\pi G)$, with $H_0 = 67 \text{ km s}^{-1} \text{ Mpc}^{-1}$ (Planck Collaboration et al. 2020).

haloes are remarkably resilient to tidal stripping (Peñarrubia et al. 2008, 2010; Errani & Navarro 2021; Amorisco 2021), and may host “micro galaxies” even after undergoing substantial tidal mass loss (Errani & Peñarrubia 2020). On the other hand, self-interacting dark matter (SIDM) or FDM models generally predict much lower dark matter densities, as a result of the inward energy transfer driven by self-interactions (SIDM) (Colín et al. 2002; Zavala et al. 2013; Tulin & Yu 2018) or of the quantum pressure support arising from the uncertainty principle (FDM) (Hu et al. 2000; Goodman 2000; Burkert 2020; Ferreira 2021).

Available data indicate that UFDs are, indeed, quite dense (see; e.g., Simon 2019; Battaglia & Nipoti 2022). This result has led recent SIDM modeling to consider much higher interaction cross sections than envisioned in earlier work (Silverman et al. 2023), in an attempt to reconcile observations with SIDM halos whose inner densities have been gravothermally enhanced by “core collapse” (Balberg et al. 2002; Nishikawa et al. 2020; Turner et al. 2021; Zeng et al. 2022). The same result places strong constraints on FDM models too, and suggests that earlier lower mass bounds for ultra-light particles based on the “classical” dwarf spheroidal (dSphs) satellites of the Milky Way should be drastically revised (Safarzadeh & Spergel 2020).

Finally, UFDs are ideal laboratories to study in unprecedented detail the heavy-element enrichment process driven by recurring episodes of star formation. Some of these galaxies are so faint and so metal poor that the abundance pattern of individual stars may well reveal the nucleosynthetic yields of individual Pop III supernovae or other explosive stellar events in these chemically pristine systems (Frebel & Norris 2015; Hansen et al. 2017; Ji et al. 2019; Marshall et al. 2019).

These traits make UFDs highly valuable, giving impetus to a number of specialized UFD searches using resolved stars in wide-field photometric surveys. Because they are so faint, UFDs are elusive objects which barely stand out against the foreground of Galactic stars and the background of distant galaxies.

UFD candidates are typically identified by match-filter techniques, which pinpoint clumps of old stars at a common distance (Koposov et al. 2008; Walsh et al. 2009; Martin et al. 2013; Drlica-Wagner et al. 2015). These clumps are then followed up with deeper photometry and spectroscopy to enable a full characterization of the system. When available, proper motions from the Gaia mission (Simon 2018; Pace & Li 2019; McConnachie & Venn 2020a,b; Li et al. 2021) can help to aid the discovery process, but at the expense of being applicable only to relatively nearby systems, given Gaia’s relatively shallow depth compared to contemporary wide-field, digital photometric surveys.

Distinguishing dark matter-dominated UFDs from self-gravitating faint star clusters is the final, perhaps most difficult hurdle, one that can only be fully overcome by securing multi-epoch line-of-sight velocities to test whether the system is a self-gravitating star cluster or a UFD bound by the presence of dark matter (Willman & Strader 2012).

For the faintest and most distant candidates, this is a most challenging task, given the few stars bright enough to obtain spectra for, the limited precision of the individual radial velocities, uncertainties from low-number statistics (Laporte et al. 2019) and the possibility that binary stars may lead to inflated values of the velocity dispersion, confusing the interpretation (Minor et al. 2010; McConnachie & Côté 2010). Although a few dozen candidate² UFDs are currently known, with total luminosities in the range $+1 > M_V > -3$ and sizes in the range 1 to 20 pc (e.g. Muñoz et al. 2012; Balbinot et al. 2013; Torrealba et al. 2019; Mau et al. 2020; Cerny et al. 2023a,b), very few of those have been conclusively identified as dark matter-dominated UFDs because of the difficulties listed above.

The most singular of these candidates is Ursa Major III/UNIONS 1 (hereafter UMa3/U1), an astonishingly faint ($M_V \sim +2.2$) stellar system with a projected half-light radius of only $R_h = 3 \pm 1$ pc recently discovered by Smith et al. (2023), hereafter S23. UMa3/U1 orbits the Milky Way on an inclined, “halo-like” orbit with pericentre $r_{\text{peri}} \approx 13$ kpc and apocentre $r_{\text{apo}} \approx 30$ kpc. Although comparable in size to globular clusters (GCs), it is ~ 10 times fainter than the faintest known GC to date (Inman & Carney 1987; Koposov et al. 2007). It is also at least ~ 10 times fainter and ~ 5 times smaller than the faintest confirmed UFDs (Belokurov et al. 2009; Geha et al. 2009; Martin et al. 2016).

S23 report a velocity dispersion for UMa3/U1 of $\sigma_{\text{los}} = 3.7^{+1.4}_{-1.0}$ km s⁻¹ on the basis of 11 likely member stars, which would imply a mass-to-light ratio of several thousands. The authors do, however, caution that the estimate of σ_{los} is very sensitive to the inclusion (or exclusion) of specific member stars: removing a single star (the largest outlier in velocity, perhaps a binary star) drops the estimate to $\sigma_{\text{los}} = 1.9^{+1.4}_{-1.1}$ km s⁻¹. Removing a second outlier from the sample results in a formally unresolved velocity dispersion, consistent with the extremely small value expected if UMa3/U1 were a self-gravitating star cluster ($\sigma_{\text{los}} \sim 50$ m/s). Should σ_{los} prove much higher than this value, it would imply that UMa3/U1 is the faintest, or “darkest” galaxy ever discovered.

Because of the sensitivity of the σ_{los} estimate to the two outliers, and because of the lack of repeat velocity measurements (to rule out the undue influence of binary stars), S23 are unable to ascertain the true nature of UMa3/U1. It is clear, however, that, regardless of its nature, this system is truly exceptional.

We present here a simple argument in favour of the interpretation of UMa3/U1 as a genuine dark matter dominated UFD. The argument relies on the fact that, should UMa3/U1 be a self-gravitating star cluster lacking dark matter, its average density would be comparable to the mean density of the Galaxy at the pericentre of its orbit. As such, it could not survive long on its current orbit, which, given the short orbital time of UMa3/U1 around the Galaxy, seems extremely unlikely.

² We colloquially refer to these systems as “glorfs”; i.e., either a dwarf galaxy or a globular cluster.

We elaborate on this idea in Sec. 2, where we use N -body simulations to model the tidal evolution of UMa3/U1, under the assumption that it is a self-gravitating star cluster. In Sec. 3, we model UMa3/U1 as a dark matter-dominated *micro-galaxy* and show that its estimated velocity dispersion is consistent with that expected if UMa3/U1 inhabits a cuspy $\sim 10^9 M_\odot$ CDM halo. Finally, we summarize and discuss our main conclusions in Sec. 4.

2. Self-gravitating (SG) model

Assuming that UMa3/U1 is a self-gravitating star cluster, we adopt a simple model where its density profile is approximated by a spherical exponential distribution,

$$\rho_\star(r) = \rho_0 \exp(-r/r_\star), \quad (1)$$

with a scale radius r_\star and a total stellar mass $M_\star = 8\pi\rho_0 r_\star^3$. The 3D and 2D half-mass radii are related to the scale radius through $r_h \approx 2.67 r_\star$ and $R_h \approx 2.02 r_\star$, respectively. The line-of-sight velocity dispersion may be computed from the projected virial theorem (Amorisco & Evans 2012; Errani et al. 2018),

$$\langle \sigma_{\text{los}}^2 \rangle = \frac{5}{96} \frac{GM_\star}{r_\star}. \quad (2)$$

Using the parameters estimated by S23, $M_\star = 16_{-5}^{+6} M_\odot$ and $R_h = (3 \pm 1)$ pc, we estimate, for the self-gravitating case, a line-of-sight velocity dispersion of

$$\sigma_{\text{los}} \equiv \langle \sigma_{\text{los}}^2 \rangle^{1/2} = 49_{-11}^{+14} \text{ m s}^{-1}. \quad (3)$$

The uncertainties above are estimated from a Monte Carlo sample, taking into account the asymmetric measurement uncertainties on M_\star and R_h . Note that a velocity dispersion this small is well below what S23 could measure given their observational setup.

Confirming that the (virial) velocity dispersion of UMa3/U1 is indeed of the order of a few km s^{-1} , as suggested from the dispersion estimate of S23 from the 10- and 11-member samples (see Sec. 1), would rule out conclusively and convincingly the possibility that this system is a self-gravitating star cluster.

2.1. Tidal evolution

2.1.1. N -body models

We use N -body simulations to analyze the evolution of the self-gravitating UMa3/U1 model described above in the MW gravitational potential. The progenitor of UMa3/U1 is modelled as a spherical N -body realisation of an exponential sphere with 10^6 particles with isotropic velocity dispersion, generated using the code described in Errani & Peñarrubia (2020), available online³. We explore models with initial masses in the range $16 \leq M_\star/M_\odot \leq 160$. All models have the same initial (2D) half-light radius of $R_h = 3$ pc.

For the Milky Way halo, we assume the static, analytical potential from Errani & Peñarrubia (2020). The potential

includes a thick and a thin axisymmetric Miyamoto & Nagai (1975) disc ($M_{\text{thick}} = 2.0 \times 10^{10} M_\odot$, $M_{\text{thin}} = 5.9 \times 10^{10} M_\odot$, radial scale lengths $a_{\text{thick}} = 4.4$ kpc, $a_{\text{thin}} = 3.9$ kpc, and vertical scale lengths $b_{\text{thick}} = 0.92$ kpc, $b_{\text{thin}} = 0.31$ kpc for the thick and thin disc, respectively), a spherical Hernquist (1990) bulge ($M_b = 2.1 \times 10^{10} M_\odot$ and scale length $a_b = 1.3$ kpc), and an NFW (Navarro et al. 1996, 1997) dark matter halo ($M_{200} = 1.15 \times 10^{12} M_\odot$, $r_{200} = 192$ kpc, and concentration $c = 9.5$), with parameters chosen to approximate the circular velocity curve of McMillan (2011). In practice, the adopted Galactic potential is not too different, in the regions of interest, from that of a singular isothermal sphere with constant circular velocity, $V_c \approx 240 \text{ km s}^{-1}$.

The integration is performed using the particle-mesh code SUPERBOX (Fellhauer et al. 2000). This code employs two cubic grids of 128^3 cells co-moving with the N -body model with resolutions 0.04 pc and 0.4 pc, respectively, as well as a fixed 128^3 cell grid containing the entire simulation volume with a lower resolution of ≈ 1.6 kpc.

2.1.2. Tidal disruption timescales

We begin by simply evolving the SG UMa3/U1 model forward from its observed present-day position and proper motions, as listed by S23. This results in an orbit with a pericentre of $r_{\text{peri}} \approx 13$ kpc, and apocentre of $r_{\text{apo}} \approx 30$ kpc. The total bound mass is shown, as a function of time, in Figure 1, where the blue diamond symbol (along the vertical dotted line labelled “now”) represents the present-day configuration of UMa3/U1. As is clear from this figure, the system fully disrupts in approximately one radial orbital time, $T_{\text{orb}} = 0.4$ Gyr.

The short survival time of the SG UMa3/U1 model is not surprising, for its mean density is comparable to the mean density of the Milky Way at the pericentre of the orbit;

$$\bar{\rho}_{\text{peri}} = 3/(4\pi G) (V_{\text{peri}}^2/r_{\text{peri}}^2) \approx 1.9 \times 10^7 M_\odot \text{ kpc}^{-3}, \quad (4)$$

where $V_{\text{peri}} \approx 240 \text{ km s}^{-1}$ (Eilers et al. 2019) is the circular velocity of the Milky Way at r_{peri} . For comparison, the mean density of the SG UMa3/U1 model within its 3D half-light radius is

$$\bar{\rho}_{\star h} = 3 M_\star / (8\pi r_h^3) = 2.9_{-1.8}^{+7.2} \times 10^7 M_\odot \text{ kpc}^{-3}, \quad (5)$$

where the quoted uncertainty takes into account the asymmetric measurement uncertainties on stellar mass M_\star and half-light radius.

To complete the analysis, we modify the initial mass of the SG UMa3/U1 model to ensure that it survives for a longer period of time on the same orbit, and adjust them to match, at present, the observed properties of UMa3/U1. Initial conditions are generated by first integrating the orbit backwards in time.

For the model to match today’s properties after evolving for, say, 12 Gyr (i.e., ~ 27 full orbits), it must have been substantially more massive/denser, as indicated by the red diamond symbol in Fig. 1. Tidal mass loss affects little the

³ <https://github.com/rerrani/nbody>

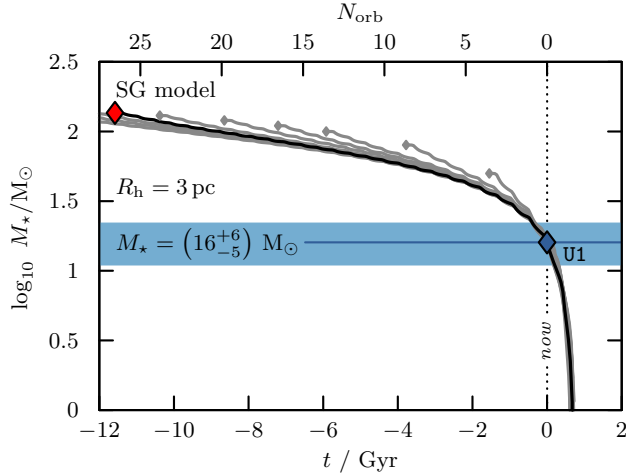


Figure 1. Mass evolution of self-gravitating N -body models for the UMa3/U1 stellar system. All models have an initial (2D) half-light radius of $R_h = 3$ pc. A blue band shows the $1\text{-}\sigma$ measurement uncertainty around the current mass of UMa3/U1. The evolution of an example model with initial mass $M_\star = 136 M_\odot$ (red diamond symbol) is highlighted in black (see text). Note that all models, independently of their initial mass, fully disrupt within ~ 0.4 Gyr from now, suggesting that if UMa3/U1 is a self-gravitating object, then we observe it at a very special point in time in its evolution.

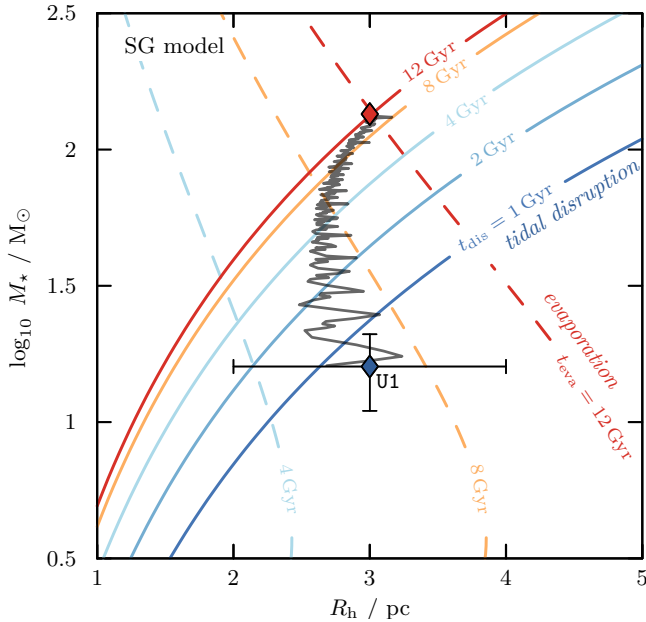


Figure 2. As Fig. 1, but for the tidal evolution in the mass-size plane. Numerical estimates of the tidal disruption (t_{dis}) and evaporation (t_{eva} , Eq. 7) timescales are shown by solid and dashed colored curves, respectively. The present-day mass and size of UMa3/U1 are shown as a blue diamond with $1\text{-}\sigma$ errorbars. A grey curve shows the evolution of the example model highlighted in Fig. 1.

size of the bound remnant, so a model with similar half-mass radius, but an initial mass of $\sim 136 M_\odot$ could, in principle, have been the progenitor of today’s UMa3/U1. The evolution of this progenitor in the mass-radius plane is shown in Fig. 2.

The coloured curves in Fig. 2 are fitted to disruption times measured in the simulations. As shown in Errani et al. (2023), on a given orbit, the disruption times depend mainly on the initial density contrast between progenitor and host, measured at pericentre. Intermediate values of the initial mass (i.e., in the range $16 \leq M_\star/M_\odot \leq 160$) lead, as expected, to intermediate survival times, as shown by the grey lines/diamonds in Fig. 1. Still, all of these models disrupt fully in less than 0.4 Gyr from now. Given that stars in UMa3/U1 are likely $\gtrsim 11$ Gyr old (S23), it would require quite the coincidence to discover UMa3/U1 just as we witness its final orbit around the Milky Way.

2.1.3. Tidal debris

However unlikely the SG UMa3/U1 model might be, a robust prediction that may be scrutinized observationally is the presence of tidal debris along the orbit. Given the extremely low velocity dispersion of the progenitor, the debris should align along a thin stream, as depicted by the red dots in the top panel of Fig. 3. The particular realization shown in this figure corresponds to the 12 Gyr-old progenitor identified by the red diamond in Fig. 1, but the configuration would be similar for other massive progenitors.

The bottom panel of Fig. 3 shows a close-up view of the present-day configuration of the simulated UMa3/U1 system, in Galactic coordinates. Because of the intrinsic faintness of the system, only a few individual stars are expected to trace the tidal tails outside the inner couple of arcminutes from the centre of the system (the half-mass radius spans roughly $1'$ at 10 kpc, the assumed distance of UMa3/U1; see S23).

We may use those stars to test the possibility that the velocity dispersion estimate of UMa3/U1 might be artificially enhanced by the presence of stars in the process of being stripped from the system. We find that the line-of-sight velocity dispersion using all stars within 1, 2, 3, and 5 half-mass radii varies by less than $\sim 20 \text{ m s}^{-1}$ from its average value of $\sim 60 \text{ m s}^{-1}$. In addition, the total line-of-sight velocity gradient across the galaxy is less than $25 \text{ m s}^{-1}/\text{arcmin}$, so that stars $6'$ ahead or behind the main body of the remnant differ by less than 300 m s^{-1} on average, a value too small to be detectable with the line-of-sight velocities of S23. These results are not unexpected given the extremely low escape velocity of the SG UMa3/U1 model, which (assuming the exponential profile of Eq. 1) is only $v_{\text{esc}} = (GM_\star/r_\star)^{1/2} \approx 215 \text{ m s}^{-1}$ at the centre. For comparison, all of the likely UMa3/U1 members with available velocity estimates identified by S23 lie within $4 R_h$ from the centre of UMa3/U1.

The velocity dispersion estimate in the self-gravitating model thus seems to depend only weakly on the radial extent over which stars are collected, and certainly does not approach in any case the few km/s estimated by S23 using 10 or 11 likely members (and neglecting binaries). We conclude that the inclusion of weakly bound stars, or of stars stirred by

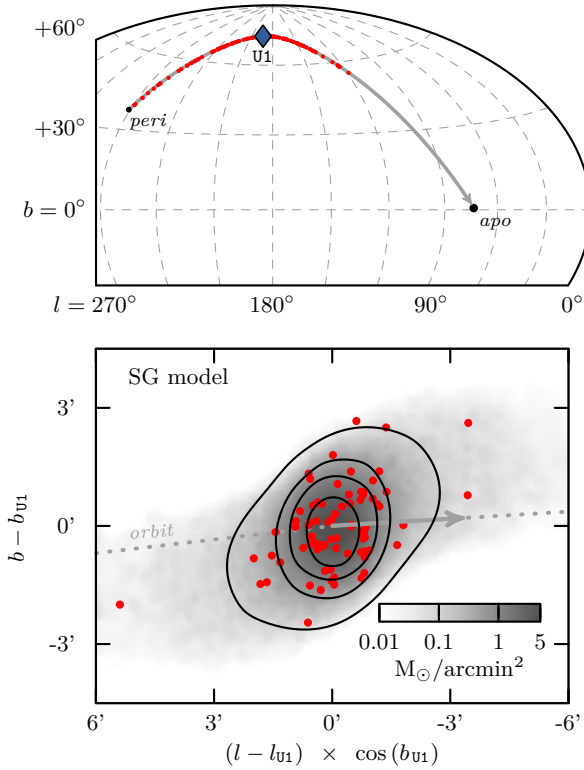


Figure 3. Top panel: orbit of UMa3/U1 in Galactic coordinates. Red points show a Monte-Carlo sample of stripped stars drawn from the N -body model highlighted in Fig. 1. Bottom panel: surface-density map of the self-gravitating model (greyscale). The orbit is shown using a dotted curve, with an arrow indicating the direction of motion along the orbit.

the Galactic tidal field, cannot explain such a high velocity dispersion estimate.

2.2. Evaporation timescales

In addition to external tidal forces, internal collisional processes may alter the structure and bound mass of a stellar system. This is especially true for a system with as few stars as UMa3/U1, which may “evaporate” due to collisions between stars in less than a Hubble time. Assuming, for simplicity, that all stars have the same mass of $\sim 0.25 M_{\odot}$, we find that UMa3/U1 has approximately $N_h \approx 2 M_{\star}/M_{\odot} \approx 32$ stars within the half-light radius. The relaxation time is related to the half-mass crossing time by (Spitzer 1987)

$$T_{\text{rel}} \approx \frac{N_h}{8 \ln N_h} T_{\text{cross}} = (48 \pm 25) \text{ Myr}, \quad (6)$$

where $T_{\text{cross}} \approx (GM_{\star}/2r_h^3)^{-1/2} = (42 \pm 22) \text{ Myr}$ for $M_{\star} = 16 M_{\odot}$ and $r_h = 4 \text{ pc}$. The uncertainties quoted here are estimated by linear propagation of the measurement uncertainties.

A rough estimate of the evaporation time scale is then given by (Binney & Tremaine 1987)

$$T_{\text{evap}} \approx 136 T_{\text{rel}} = (6.5 \pm 3.4) \text{ Gyr}. \quad (7)$$

This time scale is substantially longer than the time scale for full tidal disruption. Evaporation time estimates are shown as dashed colored curves in Fig. 2. Collisional evaporation is thus unlikely to alter our main conclusion above: the short time to full tidal disruption clearly disfavors the suggestion that UMa3/U1 is a self-gravitating star cluster.

3. Dark matter-dominated model

The simplest alternative to explain the long-term survival of UMa3/U1 in the Galactic tidal field is that UMa3/U1 is embedded in a dark matter subhalo which protects the stellar component from tidal forces. The presence of dark matter would lead to a much increased velocity dispersion compared with the self-gravitating case studied in the previous section.

As a definite example, we shall adopt below the 10-member dispersion estimate of $\sigma_{\text{los}} = 1.9^{+1.4}_{-1.1} \text{ km s}^{-1}$ reported by S23, although we note again that this value may be revised once future observations enable a proper accounting of the effect of potential binary stars. We note as well that even a lower value of the velocity dispersion would qualify UMa3/U1 as a UFD, provided that it is substantially above the $\sim 50 \text{ m/s}$ expected from the self-gravitating model.

3.1. Dynamical mass estimate

The velocity dispersion adopted above would imply a dynamical-to-stellar mass ratio comparable to the most heavily dark matter-dominated dwarfs known to date. We show this in Fig. 4, where we contrast UMa3/U1 with a compilation⁴ of dynamical and stellar masses of Local Group dwarf galaxies (squares) and globular clusters (circles) with measured kinematics. Diagonal dashed curves correspond to constant dynamical-to-stellar mass ratios, approximated by

$$\Upsilon_{\text{dyn}} \equiv \frac{M_{\text{dyn}}(< r_h)}{M_{\star}(< r_h)} \approx 8 R_h \langle \sigma_{\text{los}}^2 \rangle G^{-1} M_{\star}^{-1}. \quad (8)$$

In the above equation, we estimate the dynamical mass $M_{\text{dyn}}(< r_h)$ enclosed within the 3D half-light radius r_h from the combined measurement of line-of-sight velocity dispersion σ_{los} and 2D half-light radius R_h , with the coefficient⁵ from Wolf et al. (2010); Errani et al. (2018). The total stellar mass M_{\star} is approximated assuming a stellar mass-to-light ratio of $M_{\star}/L_V \approx 1.6$ (as in Woo et al. 2008 for galaxies with old stellar populations). Self-gravitating star clusters follow

⁴ The data shown for dwarf galaxies is as compiled in McConnachie (2012) (version January 2021, with updated data for Antlia 2 (Ji et al. 2021), Bootes 2 (Bruce et al. 2023), Crater 2 (Ji et al. 2021), Tucana (Taibi et al. 2020), Tucana 2 (Chiti et al. 2021), And 19 (Collins et al. 2020) and And 21 (Collins et al. 2021)). For globular clusters, the data is taken from Harris (1996) (version December 2010, and updated half-light radii and velocity dispersions for Pal-5 from Kuzma et al. 2015; Gieles et al. 2021; for NGC 2419 from Baumgardt et al. 2009, and for Pal-14 from Hilker 2006; Jordi et al. 2009).

⁵ For dynamical masses enclosed within the 3D half-light radius, Wolf et al. (2010) and Errani et al. (2018) give near-identical results. The derivation presented in the latter work, based on the projected virial theorem, guarantees that the results are independent of anisotropy in the velocity dispersion.

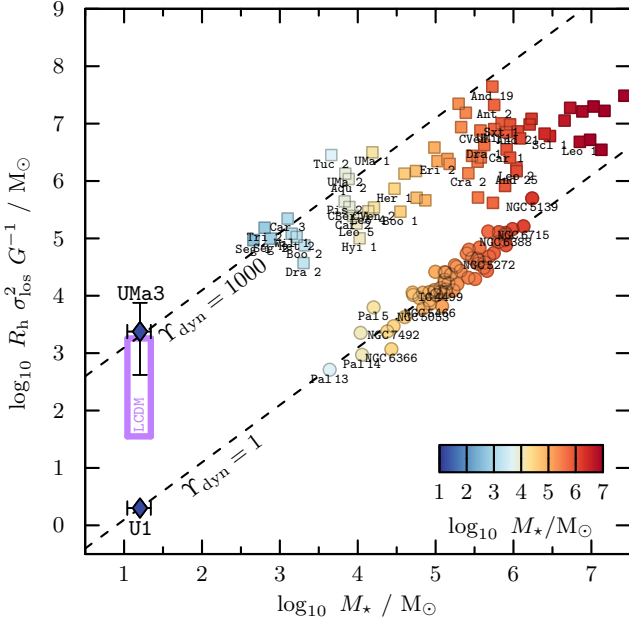


Figure 4. Dynamical mass, $R_h \sigma_{\text{los}}^2 G^{-1}$, vs stellar mass, M_* , for Local Group dwarf galaxies (squares) and globular clusters (circles). Dashed diagonal lines indicate dynamical-to-stellar mass ratios of $Y_{\text{dyn}} = 1$ and 1000, respectively (see Eq. 8 for definition). Globular clusters are distributed with little scatter around the $Y_{\text{dyn}} = 1$ line. Dwarf galaxies, whose dynamics is dominated by dark matter, lie well above that line. Taking its measured velocity dispersion at face value, UMa-3 is located well within the LCDM prediction (purple rectangle, see Sec. 3.2), whereas the self-gravitating model explored in Sec. 2, by construction, falls exactly on the $Y_{\text{dyn}} = 1$ line. References for the data shown are listed in footnote 4.

closely a line with constant dynamical-to-stellar mass ratio labelled $Y_{\text{dyn}} = 1$, whereas dwarfs are clearly offset to much higher values of the dynamical-to-stellar mass ratio.

The blue diamond at the bottom-left corner shows where UMa3/U1 would be located if it was a faint globular cluster akin to the self-gravitating (SG) model explored earlier (in which case it would be called “UNIONS 1”, or U1, for short). The other blue diamond labelled “UMA3” corresponds to adopting the 10-star dispersion $\sigma_{\text{los}} = 1.9^{+1.4}_{-1.1} \text{ km s}^{-1}$, resulting in a dynamical-to-stellar mass ratio of $Y_{\text{dyn}} = 1.2^{+2.8}_{-1.0} \times 10^3$. In this case, UMa3 sits comfortably close to the dwarf galaxy trend, extrapolated to extremely low stellar masses (i.e., extremely faint luminosities).

Assuming hereafter that UMa3/U1 is a dwarf galaxy (in which case it would be called simply “Ursa Major III” or UMa3, for short), we examine next whether it would be expected to survive the strong Galactic tidal field. We begin by comparing in Fig. 5 the mean density of the system within its half-mass radius, $\bar{\rho}_h$, with $\bar{\rho}_{\text{peri}}$, the mean density of the Galaxy at the pericentre of the orbit, shown by a horizontal dotted line segment. As discussed earlier, the “U1” symbol indicates that UMa3/U1’s density would be comparable to $\bar{\rho}_{\text{peri}}$ (and thus

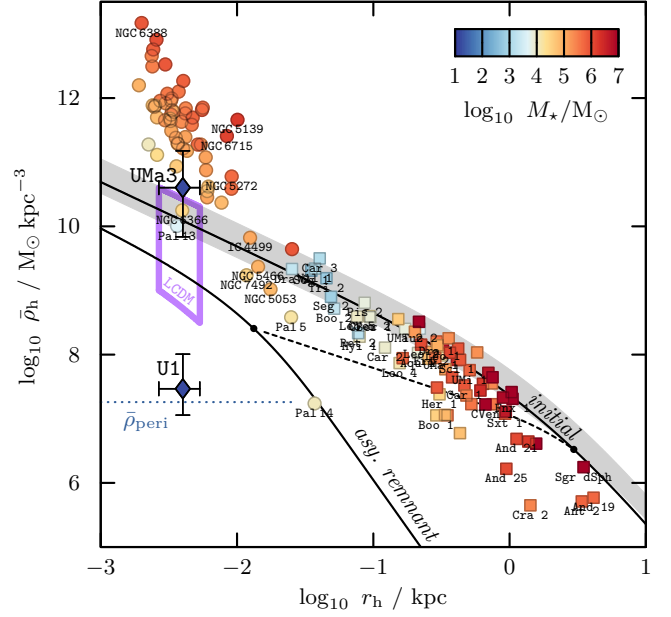


Figure 5. Mean density, $\bar{\rho}_h$, enclosed within the 3D half-light radius, r_h , for Local Group dwarf galaxies (squares) and globular clusters (filled circles), compared with UMa3/U1. The diamond labelled “U1” shows the mean density expected if UMa3/U1 is a fully self-gravitating stellar system without dark matter. The upper diamond labelled “UMA3” corresponds to adopting the measured velocity dispersion of 1.9 km s^{-1} . A grey band shows the mean densities of LCDM (NFW) haloes considered sufficiently massive to allow stars to form. A halo with a virial mass corresponding to the $z = 2$ hydrogen cooling critical mass is shown in black. The lower black curve shows the asymptotic remnants of the critical mass NFW haloes placed on the UMa3/U1 orbit. The dashed curve illustrates the “tidal track” tracing the evolution of the characteristic density and size of an NFW halo as it is stripped by tides.

doomed to rapid tidal disruption) if it was a self-gravitating cluster.

We estimate the density of UMa3 by computing the dynamical mass enclosed within its 3D half-light radius using (see footnote 5)

$$M_{\text{dyn}}(< r_h) \approx 4 R_h \langle \sigma_{\text{los}}^2 \rangle G^{-1} = \left(1.0^{+2.1}_{-0.8}\right) \times 10^4 M_{\odot}, \quad (9)$$

and dividing by the volume of a sphere of radius $r_h = (4/3) R_h$. If $\sigma_{\text{los}} = 1.9^{+1.4}_{-1.1} \text{ km/s}$, this yields

$$\bar{\rho}_h = \left(4^{+11}_{-3}\right) \times 10^{10} M_{\odot} \text{ kpc}^{-3}, \quad (10)$$

which is roughly ~ 1000 times higher than the density of the SG model, and thus safe from tidal disruption. As shown by the blue diamond labelled “UMA3” in Fig. 5, the mean density of UMa3 would in that case be comparable to that of some GCs, many of which are known to orbit the Galaxy on orbits with pericentres as small or smaller than 13 kpc.

The mean density computed above would make UMa3 not only the faintest and smallest, but also the densest UFD ever detected, with important implications for both the mass of the CDM halo inhabited by UMa3 and for alternative models of dark matter. We address these issues next.

3.2. LCDM expectations

In LCDM, galaxies form deep within the potential wells of dark matter haloes (White & Rees 1978). The ability of hydrogen gas to cool efficiently in the presence of the cosmic UV background is expected to impose a minimum *critical* halo mass below which LCDM halos are not expected to be able to host luminous galaxies.

Benitez-Llambay & Frenk (2020) argue that the critical virial mass needed to enable star formation to proceed evolves with redshift z roughly as

$$M_{\text{cr}}^z \approx (10^{10} M_{\odot}) \left[T / (3.2 \times 10^4 \text{ K}) \right]^{3/2} (1+z)^{-3/2}, \quad (11)$$

using a virial temperature of $T = 2 \times 10^4 \text{ K}$. At redshift $z = 0$, the resulting critical mass equals $M_{\text{cr}}^{z=0} \approx 4.9 \times 10^9 M_{\odot}$.

At earlier redshifts, the critical mass was somewhat lower. The best-fitting isochrone for U1/UMa3 corresponds to a stellar age of $\gtrsim 11 \text{ Gyr}$ (S23). Assuming Planck Collaboration et al. (2020) cosmological parameters, this corresponds roughly to a redshift of $z \sim 2$, which we shall adopt in what follows.

The cosmological simulations analyzed by Pereira-Wilson et al. (2023) confirm that stars first form in halos exceeding the critical mass given by eq. 11. We use their Figure 7 to estimate a range of halo masses for the potential progenitor halo of UMa3 (up to 0.5 dex above M_{cr}). Combining this with the $z = 2$ average NFW concentration (± 0.15 dex scatter) from Ludlow et al. (2016), we obtain a range of mass profiles for UMa3, which we show as a grey band in Fig. 5. The mean density profile of a halo with virial mass $M_{\text{cr}}^{z=2}$ is shown as a solid black curve within the grey band.

Fig. 5 shows that UMa3’s mass density is (for the assumed σ_{los}) comfortably within the range expected for a galaxy inhabiting a cuspy NFW halo with mass close to critical. Less massive NFW halos are less dense at all radii, and would therefore have difficulty matching UMa3’s estimated density. For example, an LCDM “mini-halo” with virial mass $10^6 M_{\odot}$ at $z = 0$ would have a mean density of $\approx 1.2 \times 10^9 M_{\odot} \text{ kpc}^{-3}$ at $r \sim 4 \text{ pc}$, well below UMa3.

The high dark matter density estimated for UMa3 thus disfavors the possibility that it may have formed at the centre of a mini-halo and supports the view that luminous galaxies, no matter how faint, only form in halos near or above the critical virial mass of Eq. 11.

If UMa3 is indeed a “micro-galaxy” (Errani & Peñarrubia 2020) formed at the centre of a cuspy NFW halo, we may use the results of Errani & Navarro (2021) and Errani et al. (2022) to predict its evolution under the influence of the Galactic tidal field. The main result of their study is that tides gradually strip a halo, approaching an asymptotic state where the characteristic density of the bound remnant equals roughly $16 \times \bar{\rho}_{\text{peri}}$. The subhalo characteristic density evolves following

a well-defined “tidal track” (Peñarrubia et al. 2008) until the asymptotic characteristic density has been reached. The bound remnant is well approximated by an “exponentially truncated” NFW profile (see Errani & Navarro 2021, for details).

The initial density profile of a halo of critical mass $M_{\text{cr}}^{z=2}$, is shown by the solid black curve in Fig. 5, labelled “initial”. This halo has a circular velocity that peaks at $V_{\text{mx}} = 23 \text{ km s}^{-1}$ at a radius $r_{\text{mx}} = 3.0 \text{ kpc}$. Its characteristic mean density at r_{mx} equals $\bar{\rho}_{\text{mx}} = 3.3 \times 10^6 M_{\odot} \text{ kpc}^{-3}$, shown as a black circle in Fig. 5. The tidal track is shown by the dashed black curve, which stops once the asymptotic remnant density of $\bar{\rho}_{\text{mx}} \approx 16 \times \bar{\rho}_{\text{peri}}$ has been reached. An exponentially truncated NFW profile (black curve labelled “asy. remnant”) illustrates the final density profile of that halo on this orbit.

We emphasize that the asymptotic remnant properties depend on those of the initial NFW halo adopted. Choosing an initial halo with a higher characteristic initial density would lead to an asymptotic remnant whose mean density, at $r = 4 \text{ pc}$, is higher. It is clear from Fig. 5 that, although Galactic tides are expected to reduce the central dark matter density of a cuspy halo, a well-characterized bound remnant is predicted to survive, whose density at radii as small as 4 pc may be as high as $\sim 10^{10} M_{\odot} / \text{kpc}^3$.

The full range of dynamical masses and densities expected at that radius in LCDM (varying halo mass and concentration) is shown by the purple curves labelled “LCDM” in Fig. 4 and Fig. 5, respectively. The corresponding range of velocity dispersions is $0.23 \lesssim \sigma_{\text{los}} / \text{km s}^{-1} \lesssim 1.1$, which is compatible with the current 10-member dispersion estimate of $\sigma_{\text{los}} = 1.9_{-1.1}^{+1.4} \text{ km s}^{-1}$ (S23). We conclude that UMa3’s properties are consistent with those expected from a micro-galaxy deeply embedded at the centre of a fairly massive, cuspy LCDM halo.

3.3. Consequences for alternative DM models

Although consistent with LCDM, the extreme properties of UMa3 inferred assuming that the 10-member velocity dispersion measurement holds ($\sigma_{\text{los}} = 1.9_{-1.1}^{+1.4} \text{ km s}^{-1}$) would be difficult to reconcile with alternative dark matter models that predict lower dark matter densities.

We begin by discussing UFDs in fuzzy dark matter (FDM) models, where the density of a dark matter-dominated UFD is thought to reflect the central density of the “solitonic core” that forms at the centre of a halo made up of ultra-light particles (Schive et al. 2014a,b; Safarzadeh & Spergel 2020). Cosmological simulations of FDM halo formation find that the central density of the core, at redshift $z = 0$, is given by (using eq. 3 and eq. 7 in Schive et al. 2014b)

$$\rho_{\text{c0}} \approx 2.9 \times 10^6 \frac{M_{\odot}}{\text{kpc}^3} \left(\frac{m_{\psi}}{10^{-22} \text{ eV}/c^2} \right)^2 \left(\frac{M_{\text{halo}}}{10^9 M_{\odot}} \right)^{4/3}, \quad (12)$$

where m_{ψ} is the mass of the ultra-light particle, and M_{halo} is a measure of the halo virial mass⁶.

⁶ The definition of halo virial mass M_{halo} and virial radius in Schive et al. (2014b) is slightly different from the one we use throughout this work (see footnote 1): at redshift $z = 0$, the mean density enclosed within the virial radius equals ≈ 350 times the mean density of the universe.

Attempts to fit the density profile of the “classical” dwarf spheroidal satellites of the MW (like Fornax or Sculptor) with a solitonic core yield upper limits for m_ψ of order 10^{-22} eV/ c^2 (Marsh & Pop 2015; González-Morales et al. 2017). This is mainly because the mean densities of Fornax and Sculptor are of order 10^7 – 10^8 M_\odot kpc $^{-3}$, consistent with eq. 12 for $M_{\text{halo}} \sim 10^{10} M_\odot$ and $m_\psi \sim 10^{-22}$ eV/ c^2 .

Achieving a density as high as that estimated for UMa3 (i.e., $\sim 4 \times 10^{10} M_\odot$ kpc $^{-3}$, see Eq. 10) would require the ultra-light particle mass to be as large as $m_\psi \sim 3 \times 10^{-21}$ eV/ c^2 (or a halo mass as large as $M_{\text{halo}} \sim 10^{12} M_\odot$, which seems rather unlikely). This choice, however, would deny the main motivation for FDM: that the presumed kpc-scale cores in dwarf galaxies suggested by some studies reflect the de Broglie wavelength of the ultra-light particle (Goodman 2000; Hu et al. 2000; Hui et al. 2017; Ferreira 2021). Reconciling FDM with the high densities of observed UFDs has already been recognized as a difficult challenge to traditional FDM models (Burkert 2020; Safarzadeh & Spergel 2020), a challenge that would become much more severe if the high density of UMa3 is confirmed by future velocity dispersion measurements.

Finally, the estimated high density of UMa3 is also difficult to accommodate with the kpc-size cores expected in self-interacting dark matter models, at least for interaction cross sections of order $1 \text{ cm}^2 \text{ g}^{-1}$ (see; e.g., Tulin & Yu 2018, and references therein). For this choice, collisions between particles erase the central cusp of a dark matter halo, creating a core with constant density that, on the scale of dwarf galaxies, do not exceed a few times $10^8 M_\odot$ kpc $^{-3}$ (Zavala et al. 2013; Vogelsberger et al. 2014). Matching the high density of UMa3 (and, indeed, of other UFDs) would require gravothermal “core collapse” to occur, raising the innermost dark matter densities to values as large as those predicted for cuspy LCDM halos, and observed in UFDs (see; e.g. Hayashi et al. 2021; Silverman et al. 2023).

The timescale for core collapse, however, likely exceeds the age of the universe for SIDM models with velocity-independent interaction cross sections (Zeng et al. 2022) (though some authors argue that the core collapse timescales may be shortened considerably by tidal effects, see Nishikawa et al. 2020). Further work is clearly needed to reconcile SIDM models with the high densities of UFDs in general, and of UMa3 in particular, should the current density estimate prove robust to binary stars.

3.4. Annihilation signals

The remarkably high density of $\bar{\rho}_h \sim 4 \times 10^{10} M_\odot \text{ kpc}^{-3}$ (Eq. 10) combined with the heliocentric distance of only (10 ± 1) kpc (S23) render UMa3/U1 an interesting target for the study of potential signals of dark matter self-annihilation. The astrophysical component to the annihilation signal for velocity-independent annihilation may be expressed through the J -factor (see e.g. Walker et al. 2011), which for stellar tracers embedded in an NFW subhalo can be estimated from (see equation 13 in Evans et al. 2016)

$$J \equiv \iint d\Omega dl \rho_{\text{NFW}}^2 \approx \frac{25}{8G^2} \frac{\sigma_{\text{los}}^4 \theta}{DR_h^2} \sim 10^{21} \frac{\text{GeV}/c^2}{\text{cm}^5}. \quad (13)$$

In the above equation, the integral is performed along the line-of-sight l over a solid angle $\Delta\Omega$, and D , R_h and σ_{los} are the heliocentric distance, projected half-light radius and line-of-sight velocity dispersion of UMa3/U1, respectively. The angle θ limits the solid angle over which the integral is computed, and is chosen here to match the Fermi-LAT resolution at GeV scales, $\theta = 0.5^\circ$ (Ackermann et al. 2014). The J -factor of $\sim 10^{21}$ GeV/ c^2 /cm 5 computed in Eq. 13 takes the measured properties of UMa3/U1 at face value. Monte-Carlo sampling of measurement uncertainties yields a 16th–84th percentile range of $10^{19} \lesssim J/(\text{GeV}/c^2/\text{cm}^5) \lesssim 10^{22}$ for the underlying distribution. Even when taking these large uncertainties into account, UMa3/U1 would be one of the “brightest” satellites of the Milky Way for potential annihilation signals, matching or exceeding the expected signal of all other known Milky Way dwarf spheroidal and ultra-faint satellites (see Tab. A2 in Pace & Strigari 2019).

4. Summary and conclusions

Ursa Major III/UNIONS 1 (UMa3/U1) is a recently-discovered satellite of the Milky Way whose extreme properties offer unique insight into the formation process of some of the faintest objects in the Universe. It is by far the faintest satellite ever discovered: at $M_V \approx +2.2$, it is ~ 10 times fainter than the faintest confirmed ultra-faint dwarfs, and ~ 10 times fainter than the least luminous globular cluster. It is also as small as some of the most compact GCs, with a projected half-mass radius of only ~ 3 pc.

Taken at face value, the line-of-sight velocity dispersion computed from the radial velocities of 10 or 11 likely members suggests the presence of dark matter (which would confirm that UMa3/U1 is indeed a dwarf galaxy). However, the lack of repeat velocity measurements and the strong dependence of the measured dispersion on the inclusion of two specific member stars leave open the possibility that UMa3/U1 is actually a self-gravitating faint cluster of stars.

The main conclusions of our work are summarized below.

(1) The orbit of the system around the Milky Way is well characterized, with a pericentric distance of only ≈ 13 kpc, an apocentric distance of ≈ 30 kpc, and a radial orbital time of ≈ 0.4 Gyr. We use N-body simulations to show that, taken its observed size and stellar mass at face value, UMa3/U1 cannot survive for longer than a single orbit if self-gravitating. Either UMa3/U1 is a GC remnant observed at a remarkably fine-tuned point in time, or it is indeed a galaxy that has survived tidal disruption because of the stabilizing effect of dark matter.

(2) The simulations do rule out the possibility that “tidal stirring” may have enhanced the observed σ_{los} to values as high as a few km/s. The models predict that, if self-gravitating, UMa3/U1 should be surrounded by a stream of tidally stripped stars, that should be searched for with high priority.

We conclude that (1) and (2) strongly support the view that UMa3/U1 is a dark matter-dominated “micro-galaxy”, indeed the faintest, or “darkest”, galaxy ever discovered.

(3) If the $\sigma_{\text{los}} = 1.9_{-1.1}^{+1.4}$ km s $^{-1}$ estimated using the 10 most-likely member stars is correct, then the mean dark matter

density for UMa3/U1 would be $\approx 4 \times 10^{10} M_{\odot} \text{ kpc}^{-3}$ within its 3D half-light radius of ~ 4 pc. This makes UMa3/U1 the densest ultra-faint galaxy known, a result that suggests that UMa3/U1 formed at the very centre of a fairly massive ($\sim 10^9$ - $10^{10} M_{\odot}$) cuspy cold dark matter halo, whose innermost regions should be able to survive the strong tidal field of the Galaxy for a Hubble time. This in turn implies a relatively high halo mass threshold for luminous galaxy formation in LCDM, as advocated by the “critical” mass model of Benitez-Llambay & Frenk (2020).

(4) If confirmed, the high dark matter density estimated for UMa3/U1 would have strong implications for alternative dark matter models. In the case of “fuzzy dark matter” (FDM), identifying it with the central density of the “solitonic core” yields an estimate for the mass of the ultra-light particle of $\sim 3 \times 10^{-21}$ eV, more than one order of magnitude higher than the 10^{-22} eV upper limits inferred in previous work (Marsh & Pop 2015; González-Morales et al. 2017). This inconsistency casts doubt on the ground motivation for FDM models, which, if confirmed, would require a re-evaluation of the model.

(5) Such a high dark matter density would also place strong constraints on SIDM models, where the dense halo cusps are eroded by collisional effects, leading to a substantial reduction

of the dark matter central densities compared to LCDM. In the context of SIDM, UMa3/U1’s central density can only be reproduced in systems that have undergone gravothermal “core collapse”, placing stringent constraints on the allowed values of the collisional cross section.

Our models show that accurate and extremely precise dispersion estimates are crucial to differentiate between UMa3/U1 being a dark matter-dominated “micro-galaxy”, or an extremely faint self-gravitating star cluster. If the current estimate of UMa3’s dynamical density is confirmed by future observations, it would not only confirm UMa3 as the “darkest” galaxy discovered to date, but it would also highlight that the predictions of LCDM seem to hold down to the faintest end of the galaxy luminosity function.

Acknowledgments

The authors would like to thank W. Cerny and T. S. Li for their helpful comments on the draft. RE acknowledges support from the European Research Council (ERC) under the European Unions Horizon 2020 research and innovation programme (grant agreement number 834148), and from the National Science Foundation (NSF) grant AST-2206046.

References

- Ackermann, M., Albert, A., Anderson, B., et al. 2014, *PhRvD*, 89, 042001, doi: [10.1103/PhysRevD.89.042001](https://doi.org/10.1103/PhysRevD.89.042001)
- Amorisco, N. C. 2021, arXiv e-prints, arXiv:2111.01148. <https://arxiv.org/abs/2111.01148>
- Amorisco, N. C., & Evans, N. W. 2012, *MNRAS*, 419, 184, doi: [10.1111/j.1365-2966.2011.19684.x](https://doi.org/10.1111/j.1365-2966.2011.19684.x)
- Balberg, S., Shapiro, S. L., & Inagaki, S. 2002, *ApJ*, 568, 475, doi: [10.1086/339038](https://doi.org/10.1086/339038)
- Balbinot, E., Santiago, B. X., da Costa, L., et al. 2013, *ApJ*, 767, 101, doi: [10.1088/0004-637X/767/2/101](https://doi.org/10.1088/0004-637X/767/2/101)
- Battaglia, G., & Nipoti, C. 2022, *Nature Astronomy*, 6, 659, doi: [10.1038/s41550-022-01638-7](https://doi.org/10.1038/s41550-022-01638-7)
- Baumgardt, H., Côté, P., Hilker, M., et al. 2009, *MNRAS*, 396, 2051, doi: [10.1111/j.1365-2966.2009.14932.x](https://doi.org/10.1111/j.1365-2966.2009.14932.x)
- Belokurov, V., Walker, M. G., Evans, N. W., et al. 2009, *MNRAS*, 397, 1748, doi: [10.1111/j.1365-2966.2009.15106.x](https://doi.org/10.1111/j.1365-2966.2009.15106.x)
- Benitez-Llambay, A., & Frenk, C. 2020, *MNRAS*, 498, 4887, doi: [10.1093/mnras/staa2698](https://doi.org/10.1093/mnras/staa2698)
- Binney, J., & Tremaine, S. 1987, *Galactic dynamics*
- Bode, P., Ostriker, J. P., & Turok, N. 2001, *ApJ*, 556, 93, doi: [10.1086/321541](https://doi.org/10.1086/321541)
- Bruce, J., Li, T. S., Pace, A. B., et al. 2023, *ApJ*, 950, 167, doi: [10.3847/1538-4357/acc943](https://doi.org/10.3847/1538-4357/acc943)
- Bullock, J. S., & Boylan-Kolchin, M. 2017, *ARA&A*, 55, 343, doi: [10.1146/annurev-astro-091916-055313](https://doi.org/10.1146/annurev-astro-091916-055313)
- Burkert, A. 2020, *ApJ*, 904, 161, doi: [10.3847/1538-4357/abb242](https://doi.org/10.3847/1538-4357/abb242)
- Cerny, W., Martínez-Vázquez, C. E., Drlica-Wagner, A., et al. 2023a, *ApJ*, 953, 1, doi: [10.3847/1538-4357/acdd78](https://doi.org/10.3847/1538-4357/acdd78)
- Cerny, W., Drlica-Wagner, A., Li, T. S., et al. 2023b, *ApJL*, 953, L21, doi: [10.3847/2041-8213/aced84](https://doi.org/10.3847/2041-8213/aced84)
- Chiti, A., Frebel, A., Simon, J. D., et al. 2021, *Nature Astronomy*, 5, 392, doi: [10.1038/s41550-020-01285-w](https://doi.org/10.1038/s41550-020-01285-w)
- Colín, P., Avila-Reese, V., Valenzuela, O., & Firmani, C. 2002, *ApJ*, 581, 777, doi: [10.1086/344259](https://doi.org/10.1086/344259)
- Collins, M. L. M., Tollerud, E. J., Rich, R. M., et al. 2020, *MNRAS*, 491, 3496, doi: [10.1093/mnras/stz3252](https://doi.org/10.1093/mnras/stz3252)
- Collins, M. L. M., Read, J. I., Ibata, R. A., et al. 2021, *MNRAS*, 505, 5686, doi: [10.1093/mnras/stab1624](https://doi.org/10.1093/mnras/stab1624)
- Drlica-Wagner, A., Bechtol, K., Rykoff, E. S., et al. 2015, *ApJ*, 813, 109, doi: [10.1088/0004-637X/813/2/109](https://doi.org/10.1088/0004-637X/813/2/109)
- Efstathiou, G. 1992, *MNRAS*, 256, 43P, doi: [10.1093/mnras/256.1.43P](https://doi.org/10.1093/mnras/256.1.43P)
- Eilers, A.-C., Hogg, D. W., Rix, H.-W., & Ness, M. K. 2019, *ApJ*, 871, 120, doi: [10.3847/1538-4357/aaf648](https://doi.org/10.3847/1538-4357/aaf648)
- Errani, R., & Navarro, J. F. 2021, *MNRAS*, 505, 18, doi: [10.1093/mnras/stab1215](https://doi.org/10.1093/mnras/stab1215)
- Errani, R., Navarro, J. F., Ibata, R., & Peñarrubia, J. 2022, *MNRAS*, 511, 6001, doi: [10.1093/mnras/stac476](https://doi.org/10.1093/mnras/stac476)
- Errani, R., Navarro, J. F., Peñarrubia, J., Famaey, B., & Ibata, R. 2023, *MNRAS*, 519, 384, doi: [10.1093/mnras/stac3499](https://doi.org/10.1093/mnras/stac3499)
- Errani, R., & Peñarrubia, J. 2020, *MNRAS*, 491, 4591, doi: [10.1093/mnras/stz3349](https://doi.org/10.1093/mnras/stz3349)

- Errani, R., Peñarrubia, J., & Walker, M. G. 2018, *MNRAS*, 481, 5073, doi: [10.1093/mnras/sty2505](https://doi.org/10.1093/mnras/sty2505)
- Evans, N. W., Sanders, J. L., & Geringer-Sameth, A. 2016, *PhRvD*, 93, 103512, doi: [10.1103/PhysRevD.93.103512](https://doi.org/10.1103/PhysRevD.93.103512)
- Fattahi, A., Navarro, J. F., Frenk, C. S., et al. 2018, *MNRAS*, 476, 3816, doi: [10.1093/mnras/sty408](https://doi.org/10.1093/mnras/sty408)
- Fellhauer, M., Kroupa, P., Baumgardt, H., et al. 2000, *NA*, 5, 305, doi: [10.1016/S1384-1076\(00\)00032-4](https://doi.org/10.1016/S1384-1076(00)00032-4)
- Ferreira, E. G. M. 2021, *A&A Rv*, 29, 7, doi: [10.1007/s00159-021-00135-6](https://doi.org/10.1007/s00159-021-00135-6)
- Ferrero, I., Abadi, M. G., Navarro, J. F., Sales, L. V., & Gurovich, S. 2012, *MNRAS*, 425, 2817, doi: [10.1111/j.1365-2966.2012.21623.x](https://doi.org/10.1111/j.1365-2966.2012.21623.x)
- Frebel, A., & Norris, J. E. 2015, *ARA&A*, 53, 631, doi: [10.1146/annurev-astro-082214-122423](https://doi.org/10.1146/annurev-astro-082214-122423)
- Geha, M., Willman, B., Simon, J. D., et al. 2009, *ApJ*, 692, 1464, doi: [10.1088/0004-637X/692/2/1464](https://doi.org/10.1088/0004-637X/692/2/1464)
- Gieles, M., Erkal, D., Antonini, F., Balbinot, E., & Peñarrubia, J. 2021, *Nature Astronomy*, 5, 957, doi: [10.1038/s41550-021-01392-2](https://doi.org/10.1038/s41550-021-01392-2)
- Gnedin, N. Y. 2000, *ApJ*, 542, 535, doi: [10.1086/317042](https://doi.org/10.1086/317042)
- González-Morales, A. X., Marsh, D. J. E., Peñarrubia, J., & Ureña-López, L. A. 2017, *MNRAS*, 472, 1346, doi: [10.1093/mnras/stx1941](https://doi.org/10.1093/mnras/stx1941)
- Goodman, J. 2000, *NewA*, 5, 103, doi: [10.1016/S1384-1076\(00\)00015-4](https://doi.org/10.1016/S1384-1076(00)00015-4)
- Hansen, T. T., Simon, J. D., Marshall, J. L., et al. 2017, *ApJ*, 838, 44, doi: [10.3847/1538-4357/aa634a](https://doi.org/10.3847/1538-4357/aa634a)
- Harris, W. E. 1996, *AJ*, 112, 1487, doi: [10.1086/118116](https://doi.org/10.1086/118116)
- Hayashi, K., Ibe, M., Kobayashi, S., Nakayama, Y., & Shirai, S. 2021, *PhRvD*, 103, 023017, doi: [10.1103/PhysRevD.103.023017](https://doi.org/10.1103/PhysRevD.103.023017)
- Hernquist, L. 1990, *ApJ*, 356, 359, doi: [10.1086/168845](https://doi.org/10.1086/168845)
- Hilker, M. 2006, *A&A*, 448, 171, doi: [10.1051/0004-6361:20054327](https://doi.org/10.1051/0004-6361:20054327)
- Hu, W., Barkana, R., & Gruzinov, A. 2000, *Physical Review Letters*, 85, 1158, doi: [10.1103/PhysRevLett.85.1158](https://doi.org/10.1103/PhysRevLett.85.1158)
- Hui, L., Ostriker, J. P., Tremaine, S., & Witten, E. 2017, *PhRvD*, 95, 043541, doi: [10.1103/PhysRevD.95.043541](https://doi.org/10.1103/PhysRevD.95.043541)
- Inman, R. T., & Carney, B. W. 1987, *AJ*, 93, 1166, doi: [10.1086/114398](https://doi.org/10.1086/114398)
- Ji, A. P., Simon, J. D., Frebel, A., Venn, K. A., & Hansen, T. T. 2019, *ApJ*, 870, 83, doi: [10.3847/1538-4357/aaf3bb](https://doi.org/10.3847/1538-4357/aaf3bb)
- Ji, A. P., Kuposov, S. E., Li, T. S., et al. 2021, *ApJ*, 921, 32, doi: [10.3847/1538-4357/ac1869](https://doi.org/10.3847/1538-4357/ac1869)
- Jordi, K., Grebel, E. K., Hilker, M., et al. 2009, *AJ*, 137, 4586, doi: [10.1088/0004-6256/137/6/4586](https://doi.org/10.1088/0004-6256/137/6/4586)
- Kuposov, S., de Jong, J. T. A., Belokurov, V., et al. 2007, *ApJ*, 669, 337, doi: [10.1086/521422](https://doi.org/10.1086/521422)
- Kuposov, S., Belokurov, V., Evans, N. W., et al. 2008, *ApJ*, 686, 279, doi: [10.1086/589911](https://doi.org/10.1086/589911)
- Kuzma, P. B., Da Costa, G. S., Keller, S. C., & Maunder, E. 2015, *MNRAS*, 446, 3297, doi: [10.1093/mnras/stu2343](https://doi.org/10.1093/mnras/stu2343)
- Laporte, C. F. P., Agnello, A., & Navarro, J. F. 2019, *MNRAS*, 484, 245, doi: [10.1093/mnras/sty2891](https://doi.org/10.1093/mnras/sty2891)
- Li, H., Hammer, F., Babusiaux, C., et al. 2021, *ApJ*, 916, 8, doi: [10.3847/1538-4357/ac0436](https://doi.org/10.3847/1538-4357/ac0436)
- Lovell, M. R., Frenk, C. S., Eke, V. R., et al. 2014, *MNRAS*, 439, 300, doi: [10.1093/mnras/stt2431](https://doi.org/10.1093/mnras/stt2431)
- Ludlow, A. D., Bose, S., Angulo, R. E., et al. 2016, *MNRAS*, 460, 1214, doi: [10.1093/mnras/stw1046](https://doi.org/10.1093/mnras/stw1046)
- Marsh, D. J. E., & Pop, A.-R. 2015, *MNRAS*, 451, 2479, doi: [10.1093/mnras/stv1050](https://doi.org/10.1093/mnras/stv1050)
- Marshall, J. L., Hansen, T., Simon, J. D., et al. 2019, *ApJ*, 882, 177, doi: [10.3847/1538-4357/ab3653](https://doi.org/10.3847/1538-4357/ab3653)
- Martin, N. F., Ibata, R. A., McConnachie, A. W., et al. 2013, *ApJ*, 776, 80, doi: [10.1088/0004-637X/776/2/80](https://doi.org/10.1088/0004-637X/776/2/80)
- Martin, N. F., Geha, M., Ibata, R. A., et al. 2016, *MNRAS*, 458, L59, doi: [10.1093/mnras/slw013](https://doi.org/10.1093/mnras/slw013)
- Mau, S., Cerny, W., Pace, A. B., et al. 2020, *ApJ*, 890, 136, doi: [10.3847/1538-4357/ab6c67](https://doi.org/10.3847/1538-4357/ab6c67)
- McConnachie, A. W. 2012, *AJ*, 144, 4, doi: [10.1088/0004-6256/144/1/4](https://doi.org/10.1088/0004-6256/144/1/4)
- McConnachie, A. W., & Côté, P. 2010, *ApJL*, 722, L209, doi: [10.1088/2041-8205/722/2/L209](https://doi.org/10.1088/2041-8205/722/2/L209)
- McConnachie, A. W., & Venn, K. A. 2020a, *Research Notes of the American Astronomical Society*, 4, 229, doi: [10.3847/2515-5172/abd18b](https://doi.org/10.3847/2515-5172/abd18b)
- , 2020b, *AJ*, 160, 124, doi: [10.3847/1538-3881/aba4ab](https://doi.org/10.3847/1538-3881/aba4ab)
- McMillan, P. J. 2011, *MNRAS*, 414, 2446, doi: [10.1111/j.1365-2966.2011.18564.x](https://doi.org/10.1111/j.1365-2966.2011.18564.x)
- Minor, Q. E., Martinez, G., Bullock, J., Kaplinghat, M., & Trainor, R. 2010, *ApJ*, 721, 1142, doi: [10.1088/0004-637X/721/2/1142](https://doi.org/10.1088/0004-637X/721/2/1142)
- Miyamoto, M., & Nagai, R. 1975, *PASJ*, 27, 533
- Muñoz, R. R., Geha, M., Côté, P., et al. 2012, *ApJL*, 753, L15, doi: [10.1088/2041-8205/753/1/L15](https://doi.org/10.1088/2041-8205/753/1/L15)
- Nadler, E. O., Drlica-Wagner, A., Bechtol, K., et al. 2021, *PhRvL*, 126, 091101, doi: [10.1103/PhysRevLett.126.091101](https://doi.org/10.1103/PhysRevLett.126.091101)
- Navarro, J. F., Frenk, C. S., & White, S. D. M. 1996, *ApJ*, 462, 563, doi: [10.1086/177173](https://doi.org/10.1086/177173)
- Navarro, J. F., Frenk, C. S., & White, S. D. M. 1997, *ApJ*, 490, 493, doi: [10.1086/304888](https://doi.org/10.1086/304888)
- Nishikawa, H., Boddy, K. K., & Kaplinghat, M. 2020, *PhRvD*, 101, 063009, doi: [10.1103/PhysRevD.101.063009](https://doi.org/10.1103/PhysRevD.101.063009)
- Pace, A. B., & Li, T. S. 2019, *ApJ*, 875, 77, doi: [10.3847/1538-4357/ab0aee](https://doi.org/10.3847/1538-4357/ab0aee)
- Pace, A. B., & Strigari, L. E. 2019, *MNRAS*, 482, 3480, doi: [10.1093/mnras/sty2839](https://doi.org/10.1093/mnras/sty2839)
- Peñarrubia, J., Benson, A. J., Walker, M. G., et al. 2010, *MNRAS*, 406, 1290, doi: [10.1111/j.1365-2966.2010.16762.x](https://doi.org/10.1111/j.1365-2966.2010.16762.x)

- Peñarrubia, J., Navarro, J. F., & McConnachie, A. W. 2008, *ApJ*, 673, 226, doi: [10.1086/523686](https://doi.org/10.1086/523686)
- Peñarrubia, J., Pontzen, A., Walker, M. G., & Koposov, S. E. 2012, *ApJL*, 759, L42, doi: [10.1088/2041-8205/759/2/L42](https://doi.org/10.1088/2041-8205/759/2/L42)
- Pereira-Wilson, M., Navarro, J. F., Benítez-Llambay, A., & Santos-Santos, I. 2023, *MNRAS*, 519, 1425, doi: [10.1093/mnras/stac3633](https://doi.org/10.1093/mnras/stac3633)
- Planck Collaboration, Aghanim, N., Akrami, Y., et al. 2020, *A&A*, 641, A6, doi: [10.1051/0004-6361/201833910](https://doi.org/10.1051/0004-6361/201833910)
- Quinn, T., Katz, N., & Efstathiou, G. 1996, *MNRAS*, 278, L49, doi: [10.1093/mnras/278.4.L49](https://doi.org/10.1093/mnras/278.4.L49)
- Safarzadeh, M., & Spergel, D. N. 2020, *ApJ*, 893, 21, doi: [10.3847/1538-4357/ab7db2](https://doi.org/10.3847/1538-4357/ab7db2)
- Sales, L. V., Wetzel, A., & Fattahi, A. 2022, *Nature Astronomy*, 6, 897, doi: [10.1038/s41550-022-01689-w](https://doi.org/10.1038/s41550-022-01689-w)
- Shive, H.-Y., Chiueh, T., & Broadhurst, T. 2014a, *Nature Physics*, 10, 496, doi: [10.1038/nphys2996](https://doi.org/10.1038/nphys2996)
- Shive, H.-Y., Liao, M.-H., Woo, T.-P., et al. 2014b, *PhRvL*, 113, 261302, doi: [10.1103/PhysRevLett.113.261302](https://doi.org/10.1103/PhysRevLett.113.261302)
- Silverman, M., Bullock, J. S., Kaplinghat, M., Robles, V. H., & Valli, M. 2023, *MNRAS*, 518, 2418, doi: [10.1093/mnras/stac3232](https://doi.org/10.1093/mnras/stac3232)
- Simon, J. D. 2018, *ApJ*, 863, 89, doi: [10.3847/1538-4357/aacdfb](https://doi.org/10.3847/1538-4357/aacdfb)
- , 2019, *ARA&A*, 57, 375, doi: [10.1146/annurev-astro-091918-104453](https://doi.org/10.1146/annurev-astro-091918-104453)
- Simon, J. D., & Geha, M. 2007, *ApJ*, 670, 313, doi: [10.1086/521816](https://doi.org/10.1086/521816)
- Smith et al. 2023, accepted manuscript, *ApJ*
- Spitzer, L. 1987, Dynamical evolution of globular clusters
- Taibi, S., Battaglia, G., Rejkuba, M., et al. 2020, *A&A*, 635, A152, doi: [10.1051/0004-6361/201937240](https://doi.org/10.1051/0004-6361/201937240)
- Torrealba, G., Belokurov, V., & Koposov, S. E. 2019, *MNRAS*, 484, 2181, doi: [10.1093/mnras/stz071](https://doi.org/10.1093/mnras/stz071)
- Tulin, S., & Yu, H.-B. 2018, *PhR*, 730, 1, doi: [10.1016/j.physrep.2017.11.004](https://doi.org/10.1016/j.physrep.2017.11.004)
- Turner, H. C., Lovell, M. R., Zavala, J., & Vogelsberger, M. 2021, *MNRAS*, 505, 5327, doi: [10.1093/mnras/stab1725](https://doi.org/10.1093/mnras/stab1725)
- Vogelsberger, M., Zavala, J., Simpson, C., & Jenkins, A. 2014, *MNRAS*, 444, 3684, doi: [10.1093/mnras/stu1713](https://doi.org/10.1093/mnras/stu1713)
- Walker, M. G., Combet, C., Hinton, J. A., Maurin, D., & Wilkinson, M. I. 2011, *ApJL*, 733, L46, doi: [10.1088/2041-8205/733/2/L46](https://doi.org/10.1088/2041-8205/733/2/L46)
- Walsh, S. M., Willman, B., & Jerjen, H. 2009, *AJ*, 137, 450, doi: [10.1088/0004-6256/137/1/450](https://doi.org/10.1088/0004-6256/137/1/450)
- White, S. D. M., & Rees, M. J. 1978, *MNRAS*, 183, 341, doi: [10.1093/mnras/183.3.341](https://doi.org/10.1093/mnras/183.3.341)
- Willman, B., & Strader, J. 2012, *AJ*, 144, 76, doi: [10.1088/0004-6256/144/3/76](https://doi.org/10.1088/0004-6256/144/3/76)
- Wolf, J., Martinez, G. D., Bullock, J. S., et al. 2010, *MNRAS*, 406, 1220, doi: [10.1111/j.1365-2966.2010.16753.x](https://doi.org/10.1111/j.1365-2966.2010.16753.x)
- Woo, J., Courteau, S., & Dekel, A. 2008, *MNRAS*, 390, 1453, doi: [10.1111/j.1365-2966.2008.13770.x](https://doi.org/10.1111/j.1365-2966.2008.13770.x)
- Zavala, J., Vogelsberger, M., & Walker, M. G. 2013, *MNRAS*, 431, L20, doi: [10.1093/mnrasl/sls053](https://doi.org/10.1093/mnrasl/sls053)
- Zeng, Z. C., Peter, A. H. G., Du, X., et al. 2022, *MNRAS*, 513, 4845, doi: [10.1093/mnras/stac1094](https://doi.org/10.1093/mnras/stac1094)